Machine Copy for Proofreading, Vol. x, y–z, 2013

MULTICONDUCTOR REDUCTION METHOD FOR MODELING CROSSTALK OF COMPLEX CABLE BUNDLES IN THE VICINITY OF A 60 DEGREE CORNER

Jian Yan[1], Zhuo Li[1, 2, *], Liangliang Liu[1], and Changqing Gu[1]

[1]College of Electronic and Information Engineering, Nanjing University of Aeronautics and Astronautics, Nanjing 210016, China

[2]State Key Laboratory of Millimeter Waves, Southeast University, Nanjing 210096, China

Abstract—This paper presents a multiconductor reduction method for modeling electromagnetic crosstalk of complex cable bundles in the vicinity of a 60 degree corner. Based on the image theory and wide separation assumption, the per-unit-length parameters of the cable bundle can be obtained analytically. A modified six-step procedure is established to define the electrical and geometrical characteristics of the reduced cable bundle model compared with the original equivalent cable bundle method (ECBM). Numerical simulations are performed to demonstrate the viability and effectiveness of the method. This work can find wide applications in real environments.

1. INTRODUCTION

With the development of electronic technology, electromagnetic (EM) environment [1–3] of electronic devices in aeronautic and automotive systems becomes more and more complex. Much electromagnetic interference (EMI) and electromagnetic compatibility (EMC) problems associated with cable bundles [4, 5] connecting these devices should be taken into consideration. In recent years, a new simplification method called ECBM [6] has been proposed which is based on the main assumption that the common-mode response is more critical than the differential-mode response when considering external EM waves coupling to cables. This effective method has been applied in the EM emissions [7, 8] and crosstalk [9, 10] of complex cable bundles over a

Received 19 December 2012.

* Corresponding author: Zhuo Li (lizhuo@nuaa.edu.cn).

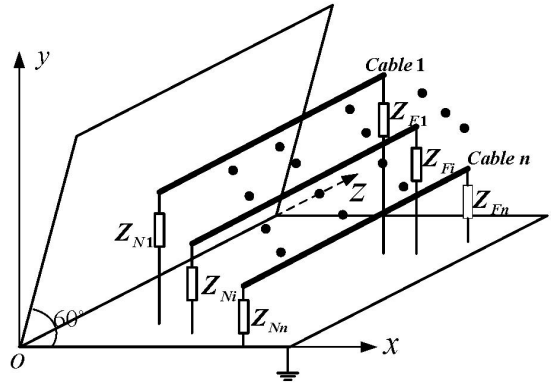

Figure 1. Illustration of n-conductor transmission lines in the vicinity of a 60 degree corner.

large frequency range with some specific adjustments. It has also been adapted to predict the crosstalk of a cable bundle in the cylindrical cavity which is considered as the ground return [11].

However, in real circumstances, cable bundles are commonly set in more complicated environments. Cable bundles in the vicinity of a corner is one of the most common environments. In practice,there are many articles about the application of transmission line [12–15]. And in this paper, we put forward a multiconductor reduction method for modeling EM crosstalk [16] of a complex cable bundle in the vicinity of a 60 degree corner. Fig. 1 shows the geometry of an n-conductor transmission lines (TL) in the vicinity of a 60 degree corner laid along the z axis and parallel to the xoz and yoz plane which are both considered as PEC ground planes, and the angle between them is 60 degrees. $Z_{N_i(F_i)}\,(i = 1, 2, \ldots, n)$ represent the near (far) end termination loads of the n-conductor TL. According to the multiconductor transmission line (MTL) and image theory [17], we can obtain the formula of the per-unit-length (p.u.l.) parameters of the cable bundle to make the ECBM fit for this new environment. Different from [11], a modified six-step procedure is established to simplify the EM crosstalk problem in this situation.

The organization of this paper is as follows. In Section 2, a modified six-step procedure is given, and the derivation and validation of the p.u.l. parameters of the cable bundle is given in detail. In Section 3, simulation results are given to validate the method, and in the final section, some comments on the proposed method are presented.

2. DERIVATION AND VALIDATION OF THE P.U.L. PARAMETERS OF MTL IN THE VICINITY OF A 60 DEGREE CORNER

2.1. Derivation of the p.u.l. Parameters

For the derivation, the following assumptions are necessary [17, 18]:

i) all conductors are PEC and the medium surrounding them is lossless;

ii) only transverse electromagnetic (TEM) mode is propagated along the conductor;

iii) the interval between each two conductors is wide enough that the charge and current distribution around each conductor can be considered as uniform.

According to the image theory [17], we can get the formula of the p.u.l. self-inductance L_{ii} of the ith conductor and mutual-inductance L_{ij} between the ith and jth conductors. Fig. 2 shows the derivation of L_{ii} and L_{ij} on the basis of the image theory.

$$\begin{aligned} L_{ii} = \frac{\psi_i}{I_i}|_{I_k=0}(k = 1 \ldots n, k \neq i) &= \frac{\mu_0}{2\pi} \ln\left(\frac{h_{1i}}{r_i}\right) + \frac{\mu_0}{2\pi} \ln\left(\frac{2h_{1i}}{h_{1i}}\right) \\ &- \frac{\mu_0}{2\pi} \ln\left(\frac{s_2}{s_1}\right) + \frac{\mu_0}{2\pi} \ln\left(\frac{s_4}{s_3}\right) + \frac{\mu_0}{2\pi} \ln\left(\frac{s_6}{s_5}\right) - \frac{\mu_0}{2\pi} \ln\left(\frac{s_7}{2h_{2i}}\right) \\ &= \frac{\mu_0}{2\pi} \ln\left(\frac{4h_{1i} \cdot h_{2i} \cdot s_1 \cdot s_4 \cdot s_6}{r_i \cdot s_2 \cdot s_3 \cdot s_5 \cdot s_7}\right), \end{aligned} \tag{1}$$

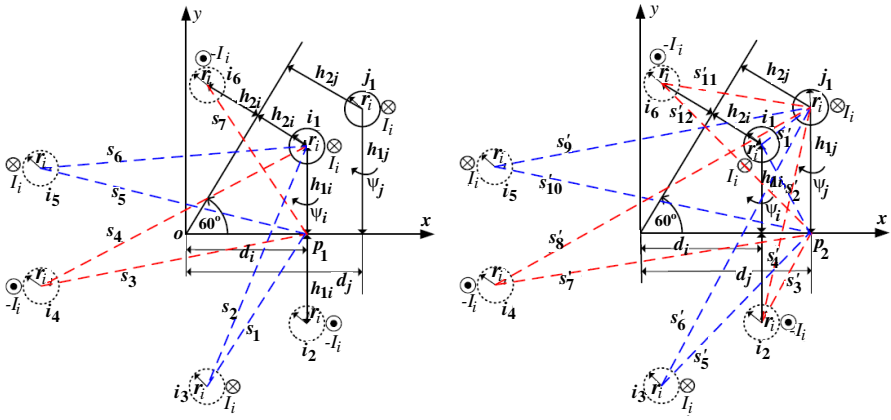

Figure 2. (a) The p.u.l. self-inductance L_{ii} of the ith conductor. (b) The p.u.l. mutual-inductance L_{ij} between the ith and jth conductors.

in which $s_1 = s_7$, $s_3 = s_6$, $h_{2i} = \dfrac{\sqrt{3}d_i - h_{1i}}{2}$ and

$$s_2 = \sqrt{(2h_{1i} + h_{2i})^2 + 3h_{2i}^2}, \tag{2}$$

$$s_4 = \sqrt{\left(\sqrt{3}h_{1i} + \sqrt{3}h_{2i}\right)^2 + (h_{1i} + h_{2i})^2}, \tag{3}$$

$$s_5 = \sqrt{\left(\sqrt{3}h_{1i} + \sqrt{3}h_{2i}\right)^2 + (h_{1i} - h_{2i})^2}, \tag{4}$$

in which $r_{i(j)}$ is the radius of the $i(j)$th conductor, conductors i_2, i_3, i_4, i_5, i_6 are the image conductors of the ith conductor, $I_{i(j)}$, $-I_{i(j)}$ are the currents flow along the $i(j)$th conductor and its image conductors, ψ_i is the magnetic flux which passes through the reference plane, $h_{1i(j)}$ represents the vertical distance between the conductor $i_1(j_1)$ and the xoz plane, $h_{2i(j)}$ represents the vertical distance between the conductor $i_1(j_1)$ and the inclined plane, d_i, d_j are the distances between the conductors i_1, j_1 and yoz plane respectively, s_1, s_3, s_5, s_7 are the distances between the image conductors i_2, i_3, i_4, i_5, i_6 and the reference point p_1 respectively, s_2, s_4, s_6 are the distances between the image conductors i_3, i_4, i_5 and conductor i_1 respectively. The formula of the mutual-inductance can be obtained as follows,

$$L_{ij} = \frac{\psi_i}{I_j}|_{I_k=0}(k = 1 \ldots n, k \neq j) = \frac{\mu_0}{2\pi}\ln\left(\frac{s_2'}{s_1'}\right) + \frac{\mu_0}{2\pi}\ln\left(\frac{s_4'}{s_3'}\right) - \frac{\mu_0}{2\pi}\ln\left(\frac{s_6'}{s_5'}\right)$$
$$+\frac{\mu_0}{2\pi}\ln\left(\frac{s_8'}{s_7'}\right) + \frac{\mu_0}{2\pi}\ln\left(\frac{s_{10}'}{s_9'}\right) - \frac{\mu_0}{2\pi}\ln\left(\frac{s_{12}'}{s_{11}'}\right) = \frac{\mu_0}{2\pi}\ln\left(\frac{s_2' \cdot s_4' \cdot s_5' \cdot s_8' \cdot s_{10}' \cdot s_{11}'}{s_1' \cdot s_3' \cdot s_6' \cdot s_7' \cdot s_9' \cdot s_{12}'}\right), \tag{5}$$

in which $s_2' = s_3'$, $s_5' = s_{12}'$, $s_7' = s_{10}'$, $d_1 = d_j - d_i$ and

$$h_{2j} = \frac{\sqrt{3}d_j - h_{1j}}{2}, \tag{6}$$

$$s_1' = \sqrt{(h_{1j} - h_{1i})^2 + d_1^2}, \tag{7}$$

$$s_4' = \sqrt{(h_{1j} + h_{1i})^2 + d_1^2}, \tag{8}$$

$$s_6' = \sqrt{(h_{1i} + h_{2i} + h_{1j})^2 + (d_1 + \sqrt{3}h_{2i})^2}, \tag{9}$$

$$s_8' = \sqrt{(h_{1j} + h_{2i})^2 + (d_1 + \sqrt{3}h_{1i} + \sqrt{3}h_{2i})^2}, \tag{10}$$

$$s_9' = \sqrt{(h_{1j} - h_{2i})^2 + (d_1 + \sqrt{3}h_{1i} + \sqrt{3}h_{2i})^2}, \tag{11}$$

$$s_{11}' = \sqrt{(h_{1j} - h_{2i} - h_{1i})^2 + (d_1 + \sqrt{3}h_{2i})^2}, \tag{12}$$

in which s'_2, s'_3, s'_5, s'_7, s'_{10}, s'_{12} are the distances between the conductors i_1, i_2, i_3, i_4, i_5, i_6 and the reference point p_2 respectively, s'_1, s'_4, s'_6, s'_8, s'_9, s'_{11} are the distances between the image conductors i_1, i_2, i_3, i_4, i_5, i_6 and conductor j_1 respectively.

2.2. Validation of the p.u.l. Parameters

In order to verify the validity of (2) and (6), we compare the results calculated from the analytical expressions with the results obtained by numerical simulations through some examples. $[L_N]$ represents the numerical results and $[L_A]$ represents the analytical one.

1) $r_i = r_j = 0.5\,\text{mm}$, $h_{1i} = 40\,\text{mm}$, $h_{1j} = 43\,\text{mm}$, $d_i = 50\,\text{mm}$, $d_j = 51\,\text{mm}$ and the p.u.l. inductance matrices (in nanohenry/meter)

$$[L_N] = \begin{bmatrix} 872.3 & 501.0 \\ & 872.5 \end{bmatrix}, \quad [L_A] = \begin{bmatrix} 868.1 & 505.1 \\ & 868.0 \end{bmatrix}. \tag{13}$$

2) $r_i = 0.5\,\text{mm}$, $r_j = 0.6\,\text{mm}$, $h_{1i} = 41\,\text{mm}$, $h_{1j} = 43\,\text{mm}$, $d_i = 50\,\text{mm}$, $d_j = 52\,\text{mm}$ and the p.u.l. inductance matrices (in nanohenry/meter)

$$[L_N] = \begin{bmatrix} 867.1 & 524.9 \\ & 838.9 \end{bmatrix}, \quad [L_A] = \begin{bmatrix} 866.4 & 523.8 \\ & 837.1 \end{bmatrix}. \tag{14}$$

Other comparison results which show excellent agreements and not reported here fully demonstrate that the analytical expressions which is based on the wide separation assumption can be accepted and introduced in the ECBM to define the electrical and geometrical characteristics of the reduced cable bundle model in the vicinity of a 60 degree corner.

3. PRESENTATION OF THE REDUCTION METHOD

In this section, a modified six-step procedure is established to simplify the EM crosstalk problem of complex cable bundles in the vicinity of a 60 degree corner. Compared with Ref. [11], Steps I, II, IV, V are identical. Thus, these steps are omitted only to avoid repetition. Only Step III is quite different and reported in detail.

Step III: Reduced Cable Bundle Cross-Section Geometry

This step is to build the reduced cable model cross-section geometry. It is realized thanks to the knowledge of the $[L_{reduced}]$ and $[C_{reduced}]$ matrices. As far as this new environment is concerned, a new optimization process made of six phase is necessary.

1) Phase 1: Estimate the hight h_{1i} and h_{2i} above the ground plane of each equivalent conductor. h_{1i} and h_{2i} correspond to the average heights of all the conductors in group i to xoz and the inclined plane.

2) Phase 2: Calculate the radius r_i of each equivalent cable according to (1)

$$r_i = \frac{2 \cdot h_{1i} \cdot h_{2i} \cdot s_4}{\exp\left(\dfrac{2\pi L_{ii\_reduced}}{\mu_0}\right) \cdot s_2 \cdot s_5}. \tag{15}$$

3) Phase 3: Calculate the distance d_{ij} between each two equivalent cables according to (5)

$$d_{ij} = \frac{s'_4 \cdot s'_8 \cdot s'_{11}}{\exp\left(\dfrac{2\pi L_{ij\_reduced}}{\mu_0}\right) \cdot s'_6 \cdot s'_9}. \tag{16}$$

4) Phase 4: Adjust r_i, d_{ij} determined by the above procedures using a dichotomic optimization realized with exact electrostatic calculations in the error range. This phase allows a reduction of the first-estimate errors involved in (15) and (16).

5) Phase 5: Determine the thickness of the dielectric coating surrounding the conductor of each equivalent cable while avoiding dielectric coating overlapping [6].

6) Phase 6: Calculate the relative permittivity ε_r of each cable dielectric coating according to the $[C_{reduced}]$ matrix using an electrostatic calculation [6].

4. VALIDATION OF THE REDUCTION METHOD FOR CROSSTALK PREDICTION THROUGH NUMERICAL SIMULATIONS

In this section, a 14-conductor point-to-point connected cable bundle, 1 m long, set in the vicinity of a 60 degree corner shown in Fig. 3(a) is investigated, in which all cables are single wire cables with the radius of 0.5 mm and surrounded by a dielectric coating with the thickness of 0.3 mm and dielectric constant of $\varepsilon_r = 2.5$ and $\mu_r = 1.0$. The distance between the two neighboring lines is 3 mm horizontally and vertically. The near end of Cable 3 (culprit cable) is excited with a periodic trapezoidal pulse voltage source shown in Fig. 4. Cable 14 serves as the victim cable. The p.u.l. parameter matrices inductance $[L]$ (in nanohenry/meter) and capacitance $[C]$ (in picoferad/meter) of the cable bundle are listed in (17) and (18). Meanwhile, in order to make the problem simpler, we only consider real loads at the two terminals of the cable bundle, which are listed in Table 1. The common-mode characteristic impedance Z_{mc} which can be determined by modal analysis [8] equals 90 Ω. According to the grouping process in Section 2, the conductors of the cable bundle can be sorted into four

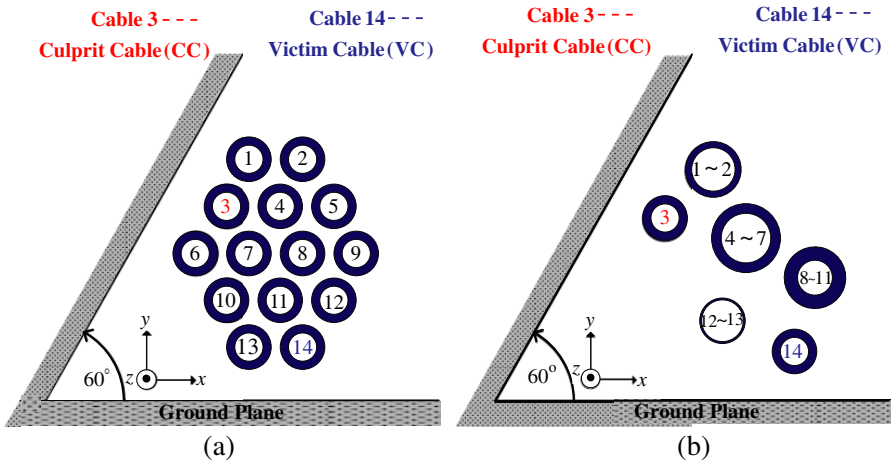

Figure 3. Cross-section geometry of (a) the complete model and (b) the reduced model.

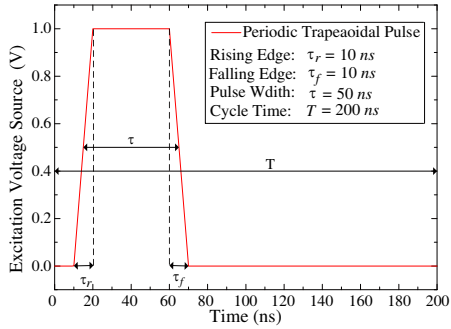

Figure 4. The trapezoidal pulse waveform of the voltage source excited on Cable 3.

groups as follows. 1) group 1: Cables $1 \sim 2$; 2) group 2: Cables $4 \sim 7$; 3) group 3: Cables $8 \sim 11$; 4) group 4: Cables $12 \sim 13$.

The p.u.l. parameter matrices $[L]$ (in nanohenry/meter) and capacitance $[C]$ (in picoferad/meter) of the reduced cable bundle model

Table 1. Termination loads of the 14-complete cable bundle model (unit: Ω).

Conductor	1	2	3	4	5	6	7
Near End	50	60	50	$1.5k$	$1.2k$	900	$1.2k$
Far End	40	28	50	$1k$	$1k$	$2k$	$1.5k$
Conductor	8	9	10	11	12	13	14
Near End	$2.3k$	$1.8k$	900	$1.2k$	55	38	50
Far End	25	30	70	48	$1.6k$	$1.5k$	100

can be easily obtained as follows [8],

$$[L]=\begin{bmatrix} 725 & 339 & 318 & 256 & 175 & 218 & 219 & 197 & 153 & 170 & 170 & 131 \\ & 786 & 348 & 371 & 164 & 226 & 266 & 264 & 163 & 196 & 212 & 150 \\ & & 783 & 392 & 239 & 349 & 371 & 304 & 230 & 269 & 267 & 200 \\ & & & 833 & 193 & 287 & 395 & 415 & 211 & 271 & 309 & 204 \\ & & & & 735 & 346 & 244 & 192 & 328 & 263 & 211 & 228 \\ & & & & & 786 & 394 & 288 & 355 & 375 & 307 & 274 \\ & & & & & & 831 & 437 & 291 & 397 & 416 & 275 \\ & & & & & & & 875 & 238 & 330 & 436 & 251 \\ & & & & & & & & 796 & 400 & 292 & 283 \\ & & & & & & & & & 836 & 439 & 403 \\ & & & & & & & & & & 876 & 334 \\ & & & & & & & & & & & 837 \end{bmatrix}_{12\times12}, \tag{17}$$

$$[C]=\begin{bmatrix} 26.4 & -7.6 & -4.4 & -0.7 & -0.5 & -0.2 & -0.1 & -0.1 & 0 & 0 & 0 & 0 \\ & 25.6 & -4.4 & -6.4 & -0.1 & -0.1 & -0.3 & -1.0 & 0 & 0 & -0.2 & 0 \\ & & 30.6 & -5.8 & -0.5 & -4.1 & -4.2 & -0.1 & 0 & -0.2 & 0 & 0 \\ & & & 27.4 & 0 & -0.4 & -4.3 & -6.4 & 0 & -0.1 & -0.6 & 0 \\ & & & & 26.4 & -5.9 & -0.2 & 0 & -6.0 & -0.5 & 0 & -0.8 \\ & & & & & 30.6 & -5.7 & -0.2 & -4.3 & -4.2 & -0.4 & -0.3 \\ & & & & & & 30.6 & -6.0 & -0.4 & -4.2 & -4.3 & -0.1 \\ & & & & & & & 25.5 & -0.1 & -0.5 & -6.5 & -0.3 \\ & & & & & & & & 27.6 & -5.8 & -0.2 & -6.3 \\ & & & & & & & & & 30.6 & -5.8 & -4.4 \\ & & & & & & & & & & 27.4 & -0.9 \\ & & & & & & & & & & & 25.4 \end{bmatrix}_{12\times12} \tag{18}$$

$$[L_{reduced}]=\begin{bmatrix} 547 & 259 & 203 & 166 \\ & 422 & 307 & 250 \\ & & 470 & 362 \\ & & & 598 \end{bmatrix}_{4\times4}, \tag{19}$$

$$[C_{reduced}]=\begin{bmatrix} 36.7 & -16.8 & -1.69 & -0.4 \\ & 81.4 & -36.8 & -2.3 \\ & & 80.3 & -28.0 \\ & & & 51.1 \end{bmatrix}_{4\times4}. \tag{20}$$

After applying the six procedures described in Section 2, we obtain the cross-section geometry of the reduced cable bundle model composed of six equivalent conductors shown in Fig. 3(b). The equivalent termination loads connected to each end of all conductors and some corresponding parameters of the reduced cable bundle are listed in Table 2.

The crosstalk voltages on the near and far ends of cable 14 can be obtained by applying the MTLN to the complete and reduced cable bundle models and are shown in Figs. 5 and 6. The comparison gives excellent agreement.

Table 2. Termination loads (unit: Ω) and some parameters (unit: mm) of the 6-reduced cable bundle model.

Conductor	1–2	3	4–7	8–11	12–13	14
Near End	27.3	50	290.3	340.7	22.5	50
Far End	16.5	50	292.7	9.2	774.2	100
Conductor Radius	1.5	0.5	2.1	2.2	1.0	0.5
Insulator Thickness	0.3	0.3	0.1	0.2	0.2	0.3

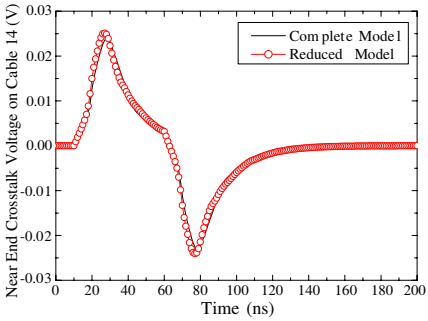

Figure 5. Comparison of the near end crosstalk voltage in the time domain on Cable 14 between the complete and reduced cable bundle models.

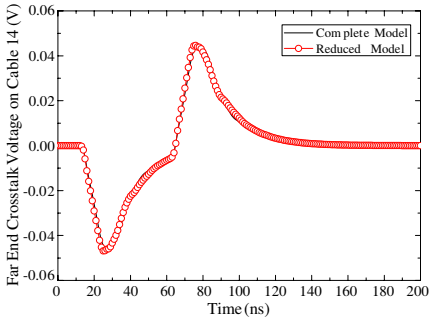

Figure 6. Comparison of the far end crosstalk voltage in the time domain on Cable 14 between the complete and reduced cable bundle models.

5. CONCLUSIONS

This paper details a modified multiconductor reduction method for a cable bundle in the vicinity of a 60 degree corner and presents a modified six-step procedure to simplify the EM crosstalk problem. The excellent agreement validates the efficiency and the advantages of the method.

In this numerical simulation, the total computation time is reduced by a factor of 4.1 (complete model costs 53 seconds, reduced model costs 13 seconds) after equivalence of the complete model by using the method of MTLN theory, which have been performed on a 2.1-GHz processor and a 2.0-GB RAM memory computer. From these results,we can show that this method can significantly reduce the prediction time and memory requirements. It could be expected that with the cable number in the original cable bundle increases, we can cut down much more computation time and memory.

ACKNOWLEDGMENT

This work was supported by the National Natural Science Foundation of China for Young Scholars under Grant No. 61102033, the Fundamental Research Funds for the Central Universities under Grant NS2012096, the Foundation of State Key Laboratory of Millimeter Waves, Southeast University, P. R. China under Grant No. K201302 and the Aeronautical Science Foundation of China under grant No. 20128052063.

REFERENCES

1. Junior, W. V., M. H. Amaral, and A. Raizer, "EMC management: How to compare electromagnetic environmental measurements and equipment immunity levels," *Progress In Electromagnetics Research Letters*, Vol. 18, 165–177, 2010.
2. Sharaa, I., D. N. Aloi, and H. P. Gerl, "EMC model-based test-setup of an electrical system," *Progress In Electromagnetics Research B*, Vol. 11, 133–154, 2009.
3. Iqbal, M. N., M. F. B. A. Malek, S. H. Ronald, M. S. Bin Mezan, K. M. Juni, and R. Chat, "A study of the EMC performance of a graded-impedance, microwave, rice-husk absorber," *Progress In Electromagnetics Research*, Vol. 131, 19–44, 2012.
4. Roy, A., S. Ghosh, and A. Chakraborty, "Simple crosstalk model of three wires to predict nearend and farend crosstalk in an EMI/EMC environment to facilitate EMI/EMC modeling," *Progress In Electromagnetics Research B*, Vol. 8, 43–58, 2008.
5. Lin, D.-B., F.-N. Wu, W. S. Liu, C. K. Wang, and H.-Y. Shih, "Crosstalk and discontinuities reduction on multi-module memory bus by particle swarm optimization," *Progress In Electromagnetics Research*, Vol. 121, 53–74, 2011.
6. Andrieu, G., L. Koné, F. Bocquet, B. Démoulin, and J. P. Parmantier, "Multiconductor reduction technique for modeling common-mode currents on cable bundles at high frequency for automotive applications," *IEEE Trans. on Electromagn. Compat.*, Vol. 50, No. 1, 175–184, Feb. 2008.
7. Andrieu, G., A. Reineix, X. Bunlon, J. P. Parmantier, L. Koné, and B. Démoulin, "Extension of the 'equivalent cable bundle method' for modeling electromagnetic emissions of complex cable bundles," *IEEE Trans. on Electromagn. Compat.*, Vol. 51, No. 1, 108–118, Feb. 2009.
8. Andrieu, G., X. Bunlon, L. Koné, J. P. Parmantier, B. Démoulin,

and A. Reineix, "The 'equivalent cable bundle method': An efficient multiconductor reduction technique to model industrial cable networks," *New Trends and Developments in Automotive System Engineering*, InTech, Jan. 2011.

9. Li, Z., L. L. Liu, and C. Q. Gu, "Generalized equivalent cable bundle method for modeling EMC issues of complex cable bundle terminated in arbitrary loads," *Progress In Electromagnetics Research*, Vol. 123, 13–30, 2012.
10. Li, Z., Z. J. Shao, J. Ding, Z. Y. Niu, and C. Q. Gu, "Extension of the 'equivalent cable bundle method' for modeling crosstalk of complex cable bundles," *IEEE Trans. on Electromagn. Compat.*, Vol. 53, No. 4, 1040–1049, Nov. 2011.
11. Li, Z., L. L. Liu, J. Ding, M. H. Cao, Z. Y. Niu, and C. Q. Gu, "A new simplification scheme for crosstalk prediction of complex cable bundles within a cylindrical cavity," *IEEE Trans. on Electromagn. Compat.*, Vol. 54, No. 4, 940–943, Aug. 2012.
12. Liu, Y., L. Tong, W. Zhu, Y. Tian, and B. Gao, "Impedance measurements of nonuniform transmission lines in time domain using an improved recursive multiple reflection computation method," *Progress In Electromagnetics Research*, Vol. 117, 149–164, 2011.
13. Miri, M. and M. McLain, "Electromagnetic radiation from unbalanced transmission lines," *Progress In Electromagnetics Research B*, Vol. 43, 129–150, 2012.
14. Yeh, Z.-Y. and Y.-C. Chiang, "A miniature CPW balun constructed with length-reduced 3 dB couples and a short redundant transmission line," *Progress In Electromagnetics Research*, Vol. 117, 195–208, 2011.
15. Deng, P.-H., J.-H. Guo, and W.-C. Kuo, "New Wilkinson power dividers based on compact stepped-impedance transmission lines and shunt open stubs," *Progress In Electromagnetics Research*, Vol. 123, 407–426, 2012.
16. Koo, S.-K., H.-S. Lee, and Y. B. Park, "Crosstalk reduction effect of asymmetric stub loaded lines," *Journal of Electromagnetic Waves and Applications*, Vol. 25, Nos. 8–9, 1156–1167, 2011.
17. Paul, C. R., *Analysis of Multiconductor Transmission Lines*, Wiley-Interscience, New York, 1994.
18. Huang, C.-C., "Analysis of multiconductor transmission lines with nonlinear terminations in frequency domain," *Journal of Electromagnetic Waves and Applications*, Vol. 19, No. 8, 1069–1083, 2005.